IMPACT OF GRADIENT-INDUCED EDDY CURRENTS ON MULTI-SHOT EPI-BASED TEMPERATURE MAP ACCURACY IN A TRANSCRANIAL MR GUIDED FOCUSED ULTRASOUND APPLICATOR

Silke M. Lechner-Greite[1], Nicolas Hehn[1], Beat Werner[2], Eyal Zadicario[3], Matthew Tarasek[4], and Desmond T.B. Yeo[4]

[1]Diagnostics, Imaging and Biomedical Technologies Laboratory, GE Global Research Europe, Garching n. Munich, Germany, [2]Center for MR-Research, Children's Hospital Zurich, Zurich, Switzerland, [3]InSightec Ltd., Tirat Carmel, Israel, [4]Diagnostics, Imaging and Biomedical Technologies Laboratory, GE Global Research Niskayuna, Albany, NY, United States

Target Audience: Researchers and engineers working in the field of transcranial magnetic resonance guided focused ultrasound (tcMRgFUS).

Purpose: Recent clinical studies have demonstrated the feasibility of tcMRgFUS surgery for brain tumors[1] and functional neurosurgery[2,3] using the ExAblate Neuro 4000 system (Insightec Ltd., Tirat Carmel, Israel) integrated into a commercial MR system (GE Signa Excite II 3.0T scanner, GE HEalthcare, Milwaukee, USA)[4]. Previous work has shown that performance of multi-plane thermal mapping using echo planar imaging (EPI) degrades with imaging artifacts caused by eddy currents induced in the transducer ground plane[5]. These distortions make accurate temperature mapping for guiding tcMRgFUS intervention very challenging. Here, the previously proposed approach of segmenting the transducer ground planes for minimizing artefacts has been refined and investigated experimentally. Spoiled gradient echo (SPGR) and EPI sequences were executed on a transducer mockup model which was based on the Alzheimer's Disease Neuroimaging Initiative phantom (ADNI, Magphan, Phantom Laboratory, Salem, NY, 2006)[6,7]. The fine structures of the ADNI phantom (typical sphere sizes are from 1 to 6cm) enables quantifying geometric distortions using regularized non-rigid registration based on a multi-resolution optical flow[8]. Additionally, a statistical evaluation performing a hypothesis test of standard deviations (std) of the temperature maps was done to compare different transducer ground plane patterns to a reference scan.

Methods: The ADNI phantom was positioned inside a 30cm diameter plastic hemisphere (Plexiglas®, 300mm diameter, flange (Zeigis)). The space between the ADNI phantom and the hemisphere was filled with demineralized water (Carl Roth GmbH, Karlsruhe, Germany) to mimic the water bolus used in the clinical transducer setup. Six different transducer ground plane segmentation patterns were realized by applying thin segmented copper sheets (Scotch 1181 3M, 10&20mm) to the outside of the plastic hemisphere (first row of Fig.1). For analysis, the transducer mockups were positioned as reproducible as possible at the iso-center of the MRI scanner. (i) 2D multiphase SPGR images for geometric distortion analysis and temperature map calculation in axial, sagittal, and coronal plane (FOV=350mm, slice thickness=4.7mm, freq × phase=144×144, TE=13.3ms, TR=26.2ms, flip angle=30°, receiver BW= ±62.5kHz, multi-phase delay time=2s), and (ii) 2D multiphase EPI images for geometric distortion analysis and temperature map calculation in axial, sagittal, and coronal plane (FOV=350mm, slice thickness=4.7mm, freq × phase=144×144, TE=13.0ms, TR=235ms, flip angle=30°, receiver BW= ±15.62.5kHz, number of shots=16, multi-phase delay time=0.5s) were acquired. The listed sequence parameters were picked such that good EPI image quality was achieved but also while remaining as close as possible to the clinical protocol. For all experiments, the transducer mockup phantom was kept at room temperature of 22°C. The integrated body coil of the MR system was used to transmit and receive the MR signal as in the clinical setup. Geometric distortions were assessed by registering the EPI images to the corresponding SPGR images[8]. The distortion maps representing pixel shifts in x and y direction were calculated for voxels with a sufficiently high contrast gradient only to avoid registering homogeneous areas. The mean and stds of the norm of the distortion vector were calculated considering equal number of voxels. Temperature maps were calculated based on the proton resonance frequency shift (PRFS) according to $\Delta T=(\varphi_T-\varphi_{T0})/(\gamma\alpha B_0 TE)$ using the phase-difference between images acquired at time T and a baseline image acquired at time T_0, with the temperature coefficient α, gyromagnetic ratio γ, B_0 and the echo times TE (13.3ms for SPGR, and 13.0ms for EPI, respectively). In total, five multi-phase images were acquired. It was found that using the fourth image as baseline image delivered stable temperature maps with respect to steady state occurrences. Both, image registration and temperature map calculation was performed using Matlab (R2013a, Mathworks Inc., Natick, MA). The temperature maps were statistically analyzed using Minitab (Minitab® Vers. 16.2.2, Minitab Inc, Coventry, UK, 2014) and the Levene/Brown-Forsythe Test performing a std equality test. To guarantee normal distribution, only regions with homogeneous temperature distribution were considered.

Results: Fig.1, the second to fourth rows, show the temperature maps inside the ADNI phantom computed from SPGR and EPI phase images, and the distortion maps for patterns a) to f) imaged in the sagittal plane, respectively. With respect to the geometric distortion analysis, map a) is representative of the geometrical difference between SPGR and EPI without induced eddy currents in the transducer ground plane. In b), c), and e) the geometric distortions show high mean values and stds compared to the reference scenario a). The star pattern in d) (3.46+/-2.33 mm) shows less distortions than the 7 segments pattern c) as used in the clinical setup (5.54+/-4.21mm). However, the combined star ring pattern achieves the best results (2.72+/-2.8mm) and image distortions are comparable to the reference scenario a) (2.77+/-2.24 mm). For SPGR, the std comparison ranked the patterns in a descending order resulting in a), d), f), c), e), and b) according to a 5% significance level. a) and d) were significantly different to the other patterns; f) differed from a) and d) and the other patterns. For EPI, the std comparison ranked the patterns in a descending order resulting in c), a), d), f), b), and e).

Discussion & Conclusion: The geometric distortion analysis of SPGR and EPI clearly demonstrates the reduction of artifacts due to eddy currents when segmenting the transducer ground plane into a star-ring pattern. Considering the mean value for the analysis proved to be difficult as the different setups were not acquired at the exact same slice location. The threshold for classifying areas with high geometric distortions was manually defined and could also have slightly influenced the results. The statistical analysis of SPGR and EPI temperature maps has shown that the temperature mean value of the selected region is not meaningful with respect to comparing two different pulse sequences. The std strongly depends on the signal to noise ratio, which is different for SPGR and EPI. The calculated temperatures from the phase images might not be affected by eddy currents, or equally affected between baseline and image at time T, but their mapping onto the imaged object is wrong due to the geometric distortions. Also, the extracted temperatures from baseline image 4 and time image 5 differ compared to temperatures calculated from baseline image 2 and 5, for example. This could be interpreted that some remaining eddy current effects have not reached a steady state yet. Future work could concentrate on considering a larger amount of phase images that go into the statistical analysis and also to acquire more initial scans before identifying a baseline image. To conclude, with this study we have demonstrated that a segmentation of the transducer ground plane into a star-ring pattern potentially could enable fast multi-plane EPI imaging for accurate MR thermometry in tcMRgFUS with geometric distortions comparable to a scenario where no copper ground plane is present, i.e. in the absence of the FUS transducer.

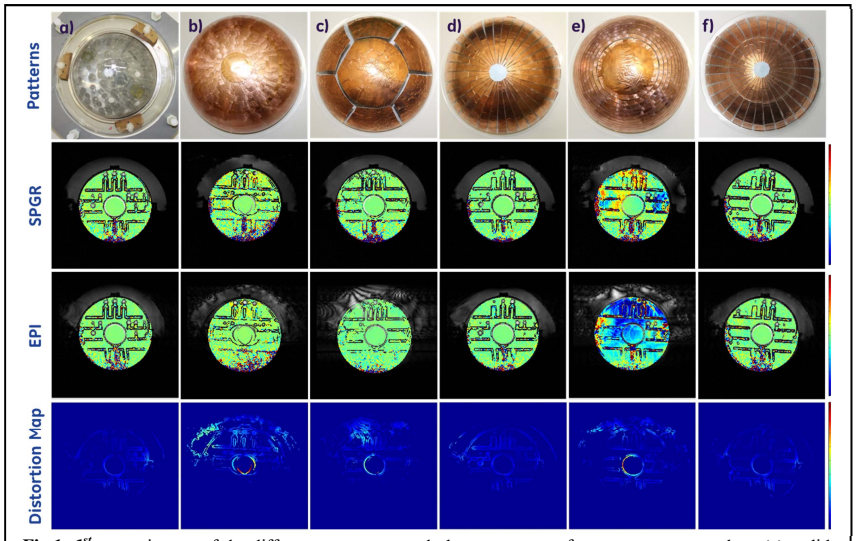

Fig.1: ***1st row:*** pictures of the different copper ground plane patterns: reference - no copper sheet (a), solid copper surface (b), 7 segments as used in clinical system (c), star pattern (d), ring pattern (e), combination of star & ring pattern (f). ***2nd row:*** Sagittal images of patterns a) to f) of SPGR with calculated temperature maps. ***3rd row:*** Sagittal images of patterns a) to f) of EPI with calculated temperature maps. ***4th row:*** Geometric distortion maps, about 5000 voxels considered in masking.

References: **1.** Coluccia et al. Journal of Therapeutic Ultrasound 2014, 2:17; **2.** Jeanmonod et al., Neurosurg Focus, 32:1–11, 2012; **3.** Elias et al., N Engl J Med, 369:640–8, 2013; **4.** Martin E et al., Ann Neurol 66:858-861 (2009); **5.** Lechner-Greite et al., Proc. 20th ISMRM, Melbourne 2012, p.1583; **6.** Mallozzi et al., Proc 14th ISMRM, Seattle 2006, p. 1364; **7.** Gunter et al., Proc 14th ISMRM, Seattle 2006, p. 2652; **8.** Lucas et al., Pro. Imaging Understanding Workshop, 1981. pp 121;